Neutron Spin Structure In the Valence Quark Region

Zein-Eddine Meziani*

Department of Physics, Temple University, Philadelphia, PA 19122

Received on 29 October, 2003

I present in this talk the latest results of the neutron spin physics program at Jefferson Laboratory in Hall A using the highly polarized electron beam and a high pressure polarized ^{3}He target. This program includes among others experiment E99-117 in which the neutron spin asymmetry A_1^n was measured in the deep inelastic region with high precision. This asymmetry is observed, for the first time, to change sign from negative to positive values between $0.3 < x < 0.6$. Furthermore we perform a flavor decomposition of the spin-dependent to spin-independent quark distributions ratios in the nucleon and find that relativistic quark models are in better agreement than pQCD fits using the hadron helicity conservation constraint as $x \to 1$.

1 Introduction

After 25 years of spin structure measurements at the high energy physics laboratories (i.e. CERN, SLAC and DESY) leading to the determination of the quark spin content of the nucleon [1, 2] and culminating with the test of the Bjorken sum rule [3], the spin structure of the neutron in the deep inelastic large x region at Q^2 (above 1 GeV^2) is still poorly measured. This region does not contribute much to the first moment of spin structure functions, but it is crucial for evaluating higher moments of these functions. These moments offer a testing ground of QCD because they are connected with specific matrix elements [4, 5] that are directly calculable in lattice QCD [6]. The spin structure function in this valence quark region can also be tested through quark model calculations.

2 Experimental method and setup

Here we present results of a precision measurement (JLab E99-117) of the neutron asymmetry A_1^n in the valence region (large $x > 0.3$ and $Q^2 > 2$GeV^2). The above experiment was carried out at Jefferson Lab in Hall A using a highly polarized electron beam (70-80%) with an average current up to $15\mu A$ and a high pressure polarized (on average between 30% and 40% in-beam) ^{3}He target with the highest polarized luminosity in the world. Details on these experiments can be found at[7]. The target is based on the spin exchange principle where rubidium atoms are polarized by optical pumping and their polarization is transferred to the ^{3}He atoms via spin exchange collisions [8]. The target was polarized either parallel or perpendicular to the direction of the electron beam and its polarization measured by three independent methods: Nuclear Magnetic Resonance (NMR) through the Adiabatic Fast Passage (AFP) technique, Electron Paramagnetic Resonance technique (EPR) and elastic scattering off ^{3}He. In each case the results of the three methods agreed within systematic errors.

The scattered electrons were detected using two high resolution spectrometers (HRS) which sat symmetrically on each side of the electron beam line to double the count rate. The spectrometers were equipped with standard detector packages which consists of two vertical drift chambers for momentum and scattering angle determination, a CO_2 gas Cherenkov counter and a double-layered lead-glass shower counter for particle identification [9]. The electron identification efficiency was 99% and the π^- rejection factor was found to be better than 10^4 for both spectrometers which was sufficient for all experiments. The momentum of each spectrometer was stepped through the relevant excitation spectrum at each incident energy of a given experiment. In many cases the comparison of the data between the two identical spectrometers at symmetric angles allowed us to minimize many of the systematic uncertainties.

3 Spin and flavor decomposition in the valence quark region

The virtual photon-nucleon asymmetry A_1^n and spin structure function g_1^n are the most poorly known in the valence quark region ($x > 0.3$). This shortcoming is due to the small scattering cross sections at large x and Q^2 combined with a lack of high polarized luminosity facilities. This region, however, is clean and unambiguous since it is not polluted by sea quarks and gluons offering thus a unique opportunity to test predictions that are difficult if not impossible at low x. The set of predictions of A_1^n in the valence quark region fall into two categories, those of relativistic consituent quark models (RCQM) which break SU(6) symmetry in the ground state wave function by hyperfine interaction [10, 11], and those of perturbative quantum chromodynaics (pQCD) with a hadron helicity conservation (HHC) constraint [12, 13] as $x \to 1$ which break SU(6) symmetry dynamically.

*For the polarized ^{3}He collaboration

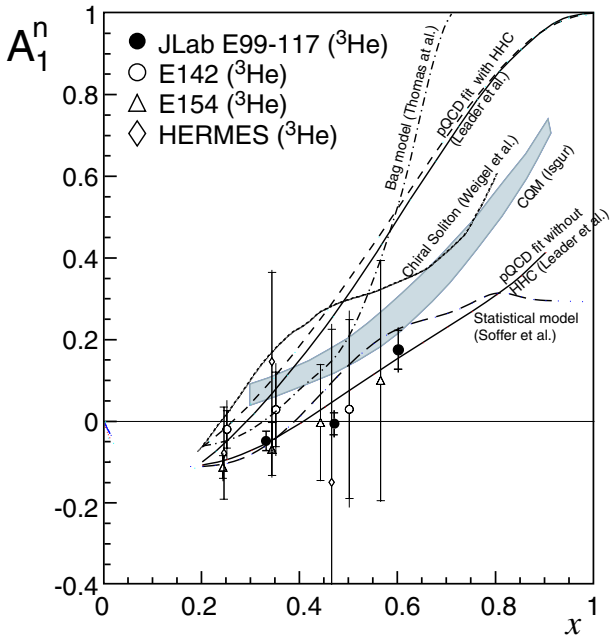

Figure 1. Left panel: Preliminary results of Jefferson Lab experiment E99-117 (solid circles) along with the world data (open symbols). We omitted world data at $x < 0.2$ for clarity. The curves are predictions described in the text.

The difference between these approaches is dramatic when the constituents flavor-spin decomposition is performed. For a proton and in the case of pQCD with HHC, we have $\Delta u(x)/u(x) \rightarrow 1$ and $\Delta d(x)/d(x) \rightarrow 1$, while for the case of RCQM's $\Delta u/u \rightarrow 1$, $\Delta d/d \rightarrow -2/3$. We notice that in leading order pQCD with HHC $\Delta d/d$ changes sign from negative at low x to positive at large x.

In Figure 1 we show preliminary results of A_1^n. The first data point at $x = 0.33$ is in good agreement with previous measurements. The data points show a clear change of sign of A_1^n as x increases and are compared with theoretical predictions. The total error in each point is dominated by the statistical error. The solid line is a prediction using HHC based on LSS(BBS) parameterization of g_1^n/F_1^n [14], the long-dashed line is a prediction of g_1^n/F_1^n from LSS 2001 parametrization at Q^2 = 5 GeV^2 without HHC constraints [15]. The shaded area is a range of predictions of A_1^n from the constituent quark model [11] while the dashed line is a calculation of the statistical model at Q^2 = 4 GeV^2 by Bourrely *et. al.* [16]. The short-dashed line is the chiral soliton model prediction at Q^2 = 3 GeV^2 by Weigel, Gamberg and Reinhardt [17]. Finally, the dot-dashed line is a bag model calculation but without meson cloud by Boros and Thomas [18] Data from Hermes and SLAC are original values without being re-analyzed for the Δ contribution of the nuclear corrections.

We used the quark parton model interpretation of g_1 and F_1 to perform a flavor decomposition of the spin dependent quark distributions assuming a negligible strange quark contribution above x = 0.3. The up-quark and down-quark distributions obtained in E99-117 (filled circles) along with preliminary results of the HERMES semi-inclusive measurements (open circles) [19] are also shown in Fig. 2. The solid line is a pQCD fit to the world data using the HHC constraint as $x \rightarrow 1$. The dashed line correspond to an RCQM prediction. It is clear that up to $x = 0.6$ the data favor the RCQM rather than the HHC pQCD based calculations. In the latter no orbital angular momentum (OAM) in considered while in the RCQM some OAM is included through the small components of the nucleon wavefunction. These results, perhaps point to the importance of considering the orbital momentum of quarks in the nucleon wave function. The dotted curve is a calculation by Wakamatsu [20] within the SU(2) chiral soliton model. The agreement of the latter with the data is quite encouraging. In the meantime, one has to wait for more measurements at larger values of x and a more complete QCD calculation.

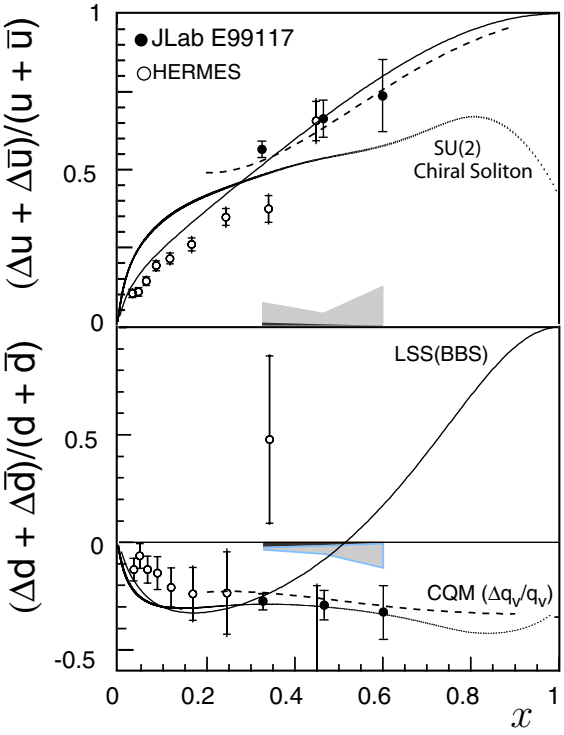

Figure 2. Spin-flavor dependent up-quark and down-quark distributions for a proton extracted from this experiment and the world data using the quark-parton model. The light error band is an estimate of the difference between the valence and the total up- and down-quark distributions including the sea. The dark band is an estimate of the strange quark contribution. The curves are predictions described in the text.

4 Conclusion

In summary, we took advantage of the highly polarized beam and high pressure polarized ^{3}He target at Jefferson Lab Hall A to investigate the internal spin structure of the neutron in the perturbative and the strong regimes of QCD. In E99-117 we have determined the world most precise down-quark helicity distribution in the valence region. The results agree with the relativistic constituent quark model and chiral soliton model rather than the HHC constrained pQCD prediction. This perhaps points to the importance of the quark OAM in this region.

Acknowledgments

I thank Roberto Ribas and the local organizers for a very well organized and productive meeting. The work presented here was supported in part with funds provided to the Nuclear and Particle Group at Temple University by the U.S. Department of Energy (DOE) under contract number DE-FG-02-94ER40844. The Southeastern Universities Research Association operates the Thomas Jefferson Accelerator Facility for the DOE under contractDE-AC05-84ER40150

References

[1] E. W. Hughes and R. Voss, Ann. Rev. Nucl. Part. Sci. **49**, 303 (1999).

[2] B. W. Filippone and X. Ji, Adv. in Nucl. Phys. **26**, 1 (2001).

[3] J. D. Bjorken, Phys. Rev. **148**, 1467 (1966); *Phys. Rev.* D **1**, 1376 (1970).

[4] E. V. Shuryak and A.I. Vainshtein, Nucl. Phys. **201**, 141 (1982).

[5] R. Jaffe and X. Ji, Phys. Rev. Lett. **67**, 552 (1991).

[6] M. Gockeler, M., et al., Phys. Rev. D **63**, 074506 (2001).

[7] Details of experiments at www.jlab.org/e99117/ and www.jlab.org/e94010/.

[8] T. G. Walker and W. Happer, Rev. Mod. Phys. **69**, 629 (1997).

[9] B. D. Anderson et al., NIM A **522**, 294 (2004).

[10] F. Close and A. W. Thomas, Phys. Lett. B **212**, 227 (1988).

[11] N. Isgur, Phys. Rev. D **59**, 034013 (1999).

[12] G. R. Farrar and A. D. Jackson, Phys. Rev. Lett. **35**, 1416 (1975).

[13] S. J. Brodsky, M. Burkhardt, and I. Schmidt, Nucl. Phys. B **441**, 197 (1995).

[14] E. Leader, A. V. Sidorov, and D. B. Stamenov, Int. J. Mod. Phys. A**13**, 5573 (1998).

[15] E. Leader, A. V. Sidorov, and D. B. Stamenov, Eur. Phys. J. C **23**, 479 (2002).

[16] C. Bourrely, J. Soffer, and F. Bucella, Eur. Phys. J. C **23**, 487 (2002).

[17] H. Weigel, and L. Gamberg, Nuc. Phys. A **680**, 48 (2000) and references therein.

[18] C. Boros and A. W. Thomas, Phys. Rev. D**60**, 074017 (1999).

[19] K. Ackerstaff et al., Phys. Lett. B**464**, 123 (1999).

[20] M. Wakamatsu, Phys. Rev. D**67**, 034005 (2003) and D**67**, 034006 (2003).